

Multifractal analysis of charged particle multiplicity distribution in the framework of Renyi entropy

Swarnapratim Bhattacharyya¹, Maria Haiduc², Alina Tania Neagu² and Elena Firu²

¹Department of Physics, New Alipore College, L Block, New Alipore, Kolkata 700053, India

Email: swarna_pratim@yahoo.com

²Institute of Space Science, Bucharest, Romania

PACS No. 25.75.-q

25.75.Ag.

25.75.Gz.

24.60.Ky.

Key words: Renyi entropy, Multiparticle Production, Multifractality, Multi fractal specific Heat

Abstract

A study of multifractality and multifractal specific heat has been carried out for the produced shower particles in nuclear emulsion detector for $^{16}\text{O-AgBr}$, $^{28}\text{Si-AgBr}$ and $^{32}\text{S-AgBr}$ interactions at 4.5A GeV/c in the framework of Renyi entropy. Experimental results have been compared with the prediction of UrQMD model. Our analysis reveals the presence of multifractality in the multiparticle production process in high energy nucleus-nucleus interactions. Degree of multifractality is found to be higher for the experimental data and it increases with the increase of projectile mass.

1. Introduction

In recent years studies of fractality emerged as an interesting research topic among the scientists [1-5]. The term Fractal was coined by Mandelbrot from the Latin word fractus which means broken or fractured [6]. Mandelbrot introduced the new geometry namely fractal geometry to look into the world of apparent irregularities. A fractal pattern is one that scales infinitely to reproduce itself such that the traditional geometry does not define it. In other words a fractal is generally a rough or fragmented geometrical shape that can be split into parts, each of which is at least approximately reduced size copy of the whole. There are many mathematical structures that are fractals e.g. Sierpinski triangle, Koch snow flake, Peano curve, Mandelbrot set and Lorentz attractor. Fractals also describe many real world objects such as clouds, mountains, turbulence and coastlines that do not correspond to simple geometrical shapes.

Fractals can be classified into two categories: multifractals and monofractals. Multifractals are more complicated self-similar objects that consist of differently weighted fractals with different non-integer dimensions. Thus the fundamental characteristic of multifractality is that the scaling properties may be different in different regions of the systems. Monofractals are those whose scaling properties are the same in different regions of the system. As the scaling properties are dissimilar in different parts of the system, multifractal systems require at least more than one scaling exponent to describe the scaling behavior of the system [7]. It should be mentioned here that the most notable property of fractals are their dimensions. Fractal dimension can be calculated by taking the limit of the quotient of the log change in object size and the log change in measurement scale, as the measurement scale approaches to zero. The differences came in what is meant by the measurement scale and how to get an average number out of many different parts of the geometrical objects. Fractal dimension quantifies the static geometry of an object. Generalized fractal dimension D_q is a well known parameter which reflects the nature of fractal structure. From the dependence of generalized fractal dimension D_q on the order q a distinguishable characterization of fractality is possible. Decrease of generalized fractal dimension D_q with the order of moment q signals the presence of multifractality. On the other hand if D_q remains constant with the increase of order q mono-fractality occurs. The study of non-statistical fluctuations by the method of scaled factorial moment leads to the presence of self-similar fractal structure in the multi-

particle production of high energy nucleus-nucleus collisions. The self-similarity observed in the power law dependence of scaled factorial moments reveals a connection between intermittency and fractality. The observed fractal structure is a consequence of self-similar cascade mechanism in multi particle production process. The close connection between intermittency and fractality prompted the scientists to study fractal nature of multiparticle production in high energy nucleus- nucleus interactions. To get both qualitative and quantitative idea concerning the multiparticle production mechanism fractality study in heavy ion collisions is expected to be very resourceful. Hwa [8] was the first to provide the idea of using multifractal moments G_q , to study the multifractality and self-similarity in multiparticle production. If the particle production process exhibits self-similar behavior also the G_q moments show a remarkable power law dependence on phase space bin size. However, if the multiplicity is low, the G_q moments are found to be dominated by statistical fluctuations. In order to suppress the statistical contribution, a modified form of G_q moments in terms of the step function was suggested by Hwa and Pan [9]. Takagi [10] also proposed a new method for studying the multifractal structure of multiparticle production. It has been pointed out by Takagi that the deviations from the linear behaviour in a log-log plot may be partly due to the fact that the above methods are unable to give the required mathematical limit, the number of points tending to infinity.

Both the G_q and the T_q techniques have been applied extensively to analyze several high-energy nucleus-nucleus interaction data [11-20]. Very recently some sophisticated methods have also been applied to study the fractal nature of multiparticle production process [21-32]. Study of multiplicity distribution and entropy of produced particles in high energy nucleus-nucleus collisions has become a subject of interest recently. Apart from studying the well known Shannon entropy, people are interested to explore the hidden physics of Renyi entropy [33-35] as well, mainly motivated by the inspiration of A. Białas and W. Czyż [36-38]. Renyi entropies are closely related with the thermodynamic entropy of the system, the Shannon entropy. Renyi entropy of different order contains information on the multiplicity moments and would serve as a useful tool for investigating the multifractal characteristics of particle production [39-40]. The advantage of this method of multifractal studies is that it is not related to the width and resolution of the phase space interval. Renyi entropy of order q can be defined as given in [36-38]

$$H_q = \frac{1}{1-q} \ln C_q \dots\dots\dots(1)$$

In terms of the probability of multiplicity distribution P_n , the values of C_q can be written as given in [36-38]

$$C_q = \sum_n (P_n)^q \dots\dots\dots(2)$$

Generalized Fractal dimension D_q can be evaluated from the concept of Renyi entropy according to the relation $D_q = \frac{H_q}{Y_m} \dots\dots(3)$

where Y_m is the central rapidity values in the centre of mass frame and is given by $Y_m = \ln[(\sqrt{s} - 2m_n \langle n_p \rangle / m_\pi)] \dots\dots\dots(4)$.

The generalized fractal dimension D_q is related with the anomalous fractal dimension d_q by a simple mathematical relation $d_q = 1 - D_q \dots\dots\dots(5)$.

Here \sqrt{s} is the centre of mass energy of the concerned collision process, m_π is the rest mass of pions, $\langle n_p \rangle$ denotes the average number of participating nucleons.

Goal of our present study is to carry out an investigation of multifractality and multifractal specific heat in shower particle multiplicity distribution from the concept of Renyi entropy measurements in ^{16}O -AgBr, ^{28}Si -AgBr and ^{32}S -AgBr interactions at 4.5 AGeV/c. We have compared our experimental results with the prediction of UrQMD model.

2. Experimental Details

In this paper, data obtained from nuclear emulsion track detector has been used for the analysis. Nuclear emulsion technique is based on the recording of tracks of each ionizing particles in photographic emulsion. Nuclear emulsion detectors offer a good angular resolution ($\sim 0.1\text{mrad}$) and they are capable of registering all the produced particles in the 4π geometry [41]. Possessing a complete 4π detector with a very good angular resolution, nuclear emulsion detectors are well suited both for investigation of event topology and for the measurements of angular distribution of different kinds of emitted or produced particles in high energy nucleus-nucleus interactions.

In order to get the required data for the present analysis, stacks of NIKFI-BR2 emulsion pellicles of dimension $20\text{cm} \times 10\text{cm} \times 600\mu\text{m}$ were irradiated by the ^{16}O , ^{28}Si and ^{32}S beam at 4.5 AGeV/c obtained from the Synchrophasatron at the Joint Institute of Nuclear Research

(JINR), Dubna, Russia [41]. The emulsion pellicles were exposed horizontally to the incoming projectile beams. When a projectile collides with the target present in nuclear emulsion an interaction or an event occurs. In order to find an interaction or an event we have scanned the emulsion plate along the track of the incident beam starting from the entry point of the beam into the emulsion plate until an interaction occurs [41]. We have also performed the scanning slowly in the backward direction from the interaction point along the track of the incident beam to ensure that the interaction selected by forward scanning did not include interaction from the secondary tracks of other interactions. Thus we have selected the primary interactions only and excluded the secondary ones from our consideration. Scanning in the forward and backward directions by two different observers increases the efficiency of selecting a primary event up to 99%. It has been mentioned in [42-43] that “along the track” scanning method gives reliable event samples because of its high detection efficiency.

2.1 Characteristics of emitted and produced particles in nuclear emulsion

According to the Powell, particles emitted from an interaction are classified into three categories, namely the shower particles, the grey particles, the black particles and the projectile fragments [41]. Characteristics of these particles are given below.

Shower particles: The tracks of particles having ionization I less or equal to $1.4I_0$ are called shower tracks. I_0 is the minimum ionization of a singly charged particle. The shower particles are mostly pions (about more than 90%) with a small admixture of kaons and hyperons (less than 10%). These shower particles are produced in a forward cone. The velocities of these particles are greater than $0.7c$ where c is the velocity of light in free space. Because of such a high velocity, these particles are not generally confined within the emulsion pellicle. Energies of these shower particles lie in the GeV range.

Grey particles: Grey particles are mainly fast target recoil protons with energies up to 400 MeV. They have ionization $1.4 I_0 \leq I < 10 I_0$. Ranges of these particles are greater than 3 mm in the emulsion medium. These grey particles have the velocities lying between $0.3c$ and $0.7c$.

Black particles: Black particles consist of both singly and multiply charged fragments. They are fragments of various elements like carbon, lithium, beryllium etc with ionization greater or equal to $10I_0$. These black particles have the maximum ionizing power. They are less energetic and consequently they are short ranged. In the emulsion medium, ranges of black particles

are less than 3 mm. The velocities of the black particles are less than $0.3c$. In emulsion experiments, it is very difficult to measure the charges of the target fragments. Therefore, it is not possible to identify the exact nucleus.

Projectile Fragments: The projectile fragments are the spectator parts of the incident projectile nucleus that do not directly participate in an interaction. They are emitted within a very narrow extremely forward cone whose semi-vertex angle ($\theta_f = 0.21/p_{inc}$) is determined by the Fermi momenta of the nucleons present in the nucleus. The value of Fermi momentum for the nucleons of the projectile is $0.21\text{GeV}/c$ [44-45]. Having almost the same energy or momentum per nucleon as the incident projectile, these fragments exhibit uniform ionization over a long range and suffer negligible scattering.

After finding the primary inelastic interactions induced by the incoming projectiles, the number of black, grey, shower tracks and the number of projectile fragments were counted for all the events of each interactions using oil immersion objectives at a total magnification of $750\times$ of a special microscope KSM (*Kernspurmessmikroskop*) made by Karl Zeiss Jena [41]. Here it should be mentioned that the present analysis is confined to the shower tracks only.

2.2 Identification of target

Nuclear emulsion medium consists of variety of nuclei like H, C, N, O, Ag and Br. It has been pointed out in [41] that in emulsion experiment, it is very difficult to measure the charges of the fragments emitted from the target and hence exact identification of the target is not possible. However, we can divide the major constituent elements present in the emulsion into three broad target groups namely hydrogen (H), light nuclei (CNO) and heavy nuclei (AgBr) on the basis of the heavy tracks (N_h) as discussed in [41]. The black and the grey tracks are collectively called the heavily ionizing tracks and the number of such tracks in an event is represented by N_h . Number of heavy tracks in an interaction is an important parameter and it helps in separating the events occurring due to the collisions of the projectile beam with the different types of target group present in emulsion medium [41]. Usually events with $N_h \leq 1$ have occurred because of the collision between hydrogen nucleus and the projectile beam [41]. This is because, when hydrogen nucleus is the target, on fragmentation the only proton will be emitted. Events with $2 \leq N_h \leq 8$ are due to collisions of the projectile beam with the

light nuclei (CNO) [41]. In case of interactions of the projectile beam with the light nuclei (CNO), it is evident that maximum number of heavy tracks cannot exceed eight. This corresponds to the largest charge of the light nucleus-the oxygen nucleus. Events with $N_h > 8$ are due to collisions of the projectile beam with the heavy target (AgBr) [41]. It can easily be understood that when $N_h > 8$, it can be ascertained that the projectile has collided with such a target whose atomic number is greater than eight. It is clear that in this case, the target cannot be of the light target group (CNO). It will be the heavy target group (AgBr). In this way by counting the number of heavy tracks, one can determine the target group.

Now one point should be mentioned. This method of target identification has some limitations in identifying the CNO target. Although the method is quite accurate in identifying the AgBr target. We have earlier said those events with $2 \leq N_h \leq 8$ are due to collisions of the projectile beam with the light nuclei (CNO). However, when $2 \leq N_h \leq 8$, there is also a possibility of events generated from peripheral collisions between the projectile and AgBr target. Therefore, in this case, the events could be an admixture of CNO events and peripheral AgBr events.

So following the method of target identification as discussed, total number of inelastic interactions can be divided into three target groups H, CNO and AgBr. For the present analysis we have not considered the events which are found to occur due to collisions of the projectile beam with H and CNO target present in nuclear emulsion. Our analysis has been carried out for the interactions of three different projectile ^{16}O , ^{28}Si and ^{32}S at 4.5 AGeV/c with the AgBr target only. Applying the selection criteria of selecting AgBr events we have chosen 1057 events of ^{16}O -AgBr interactions, 514 events of ^{28}Si -AgBr and 434 events of ^{32}S -AgBr interactions at 4.5 AGeV/c [41]. Average multiplicities of shower tracks of each interaction have been calculated and presented in table 1.

3. Analysis and Results

In a very recent paper [46] we have investigated the Renyi entropy of shower particles using ^{16}O , ^{28}Si and ^{32}S projectiles on interaction with AgBr and CNO target present in nuclear emulsion at an incident momentum of 4.5 AGeV/c. In this paper we have extended our analysis of Renyi entropy to multifractality in ^{16}O -AgBr, ^{28}Si -AgBr and ^{32}S -AgBr interactions at 4.5 AGeV/c. In order to study the fractal nature of multiparticle production from the concept

of Renyi entropy we have calculated the Renyi entropy values of order $q=2-5$ from the relation (1) and (2) for all the three interactions. The calculated values of Renyi entropy of the produced shower particles in $^{16}\text{O-AgBr}$, $^{28}\text{Si-AgBr}$ and $^{32}\text{S-AgBr}$ interactions at 4.5A GeV/c have been presented in table 2. From the table it can be noted that for all the interactions Renyi Entropy values are found to decrease as the order number increases. The variation of Renyi entropy H_q with order q has been presented in figure 1 for $^{16}\text{O-AgBr}$, $^{28}\text{Si-AgBr}$ and $^{32}\text{S-AgBr}$ interactions. Error bars drawn to every experimental point are statistical errors only. Using equation (3) and (4) we have calculated the values of generalized fractal dimension D_q for $^{16}\text{O-AgBr}$, $^{28}\text{Si-AgBr}$ and $^{32}\text{S-AgBr}$ interactions. Calculated values of generalized fractal dimension D_q for $^{16}\text{O-AgBr}$, $^{28}\text{Si-AgBr}$ and $^{32}\text{S-AgBr}$ interactions have been presented in table 3. From the table it may be noted that the values of generalized fractal dimension D_q decreases with the increase of order number suggesting the presence of multifractality in multipion production mechanism. From the table 3 it may also be noted that the values of the generalized Fractal dimension remain almost the same within the experimental error for $^{16}\text{O-AgBr}$, and $^{28}\text{Si-AgBr}$ interactions. But for $^{32}\text{S-AgBr}$ interactions the D_q values are higher in comparison to the other three interactions. The variation of D_q against the order q has been shown in figure 2 for $^{16}\text{O-AgBr}$, $^{28}\text{Si-AgBr}$ and $^{32}\text{S-AgBr}$ interactions. We have also calculated the values of ratio of $\frac{d_q}{d_2}$ for all the three interactions and presented the values in table 4. It has been pointed out in [47] that higher order bunching parameters can be expressed in terms of lower order parameters resulting a linear expression for the anomalous fractal dimension.

$$d_q = (1 - r)d_2 + \frac{q}{2}d_2r \dots\dots\dots(6)$$

$$\text{So that } \frac{d_q}{d_2} = (1 - r) + \frac{qr}{2} \dots\dots\dots(7)$$

A non zero value of the r implies the multifractal behaviour. We have plotted the variation of $\frac{d_q}{d_2}$ against the order number q in figure 3 for $^{16}\text{O-AgBr}$, $^{28}\text{Si-AgBr}$ and $^{32}\text{S-AgBr}$ interactions. The calculated values of r from the slope parameter have been presented in table 5 for our data. The value of r signifies the degree of multifractality. From the table it may be seen that for all the interactions the r value is greater than zero. This reconfirms the multifractal nature of multiparticle production mechanism. Moreover, r value characterizing the degree of multifractality is found to depend on the mass number of the projectile beam.

In thermodynamics the constant specific heat (CSH) approximation is widely applicable in many important cases; for example, the specific heat of gases and solids is constant, independent of temperature over a greater or smaller temperature interval [48]. This approximation is also applicable to multifractal data of multiparticle production processes proposed by Bershadskii [49], who introduced a multifractal Bernoulli distribution. This distribution appears in a natural way at the morphological phase transition from monofractality to multifractality as a consequence of spontaneous breaking of dimensional invariance, and it is also believed to play a crucial role in multiparticle production at higher energies. The relation for the multifractal Bernoulli function is given by $D_q = D_\infty + \frac{C \ln q}{(q-1)}$. The slope C in the above equation can be interpreted as the multifractal specific heat of the system provided that the thermodynamical interpretation of multifractality is used [50]. The gap at the multifractal specific heat at the multifractality monofractality transition allows us to consider this transition as a thermodynamic phase transition [51-52].

We have calculated the multifractal specific heat of the produced particles for ^{16}O -AgBr, ^{28}Si -AgBr and ^{32}S -AgBr interactions using relation $D_q = D_\infty + \frac{C \ln q}{(q-1)}$. The plot of D_q against $\frac{\ln q}{(q-1)}$ is shown in figure 4 for ^{16}O -AgBr, ^{28}Si -AgBr and ^{32}S -AgBr interactions. We have performed linear best fits for all the interactions. The scattered points of the figures represent the data and the lines represent the best fits. The slopes of the best linear fits of the data-sets of figure 4 give the values of specific heats (C) for all the interactions. The linear behavior in figure 4 indicates approximately good agreement between the experimental data and the multifractal Bernoulli representation. The calculated values of the multifractal specific heat for all the three interactions have been presented in table 6.

The experimental results have been compared with those obtained by analyzing events generated by the Ultra Relativistic Quantum Molecular Dynamics (UrQMD) model. UrQMD model is a microscopic transport theory, based on the covariant propagation of all the hadrons on the classical trajectories in combination with stochastic binary scattering, color string formation and resonance decay. It represents a Monte Carlo solution of a large set of coupled partial integro-differential equations for the time evolution of various phase space densities. The main ingredients of the model are the cross sections of binary reactions, the two-body potentials and decay widths of resonances. The UrQMD collision term contains 55 different baryon species (including nucleon, delta and hyperon resonances with masses up to

2.25 GeV/c²) and 32 different meson species (including strange meson resonances), which are supplemented by their corresponding anti-particle and all isospin-projected states. The states can either be produced in string decays, s-channel collisions or resonance decays. This model can be used in the entire available range of energies from the Bevalac region to RHIC to simulate nucleus- nucleus interactions. For more details about this model, readers are requested to consult [53-54]. We have generated a large sample of events using the UrQMD code (UrQMD 3.3p1) for ¹⁶O-AgBr, ²⁸Si-AgBr and ³²S-AgBr interactions at 4.5A GeV/c. We have also calculated the average multiplicities of the shower tracks for all the three interactions in case of the UrQMD data sample. Average multiplicities of the shower tracks in case of UrQMD data sample have been presented in table 1 along with the average multiplicity values of shower particles in the case of the experimental events. Table 1 shows that the average multiplicities of the shower tracks for the UrQMD events are comparable with those of the experimental values for all the interactions. We have calculated the values of Renyi entropy of order q=2-5 for all the three interactions using the UrQMD simulated data. The calculated values of Renyi entropy has been presented in table 2 along with the experimental values. From the table it may be seen that the experimentally calculated values of Renyi entropy are higher than those of their UrQMD counterparts signifies the presence of more disorderness for the experimental data. The variation of H_q with order q for the UrQMD simulated data have been presented in figure 1 along with the experimental plots for each interaction. For the UrQMD simulated events we have calculated the values of the generalized fractal dimension D_q from the values of Renyi entropy as discussed earlier. The calculated values of generalized fractal dimension for the UrQMD simulated events of ¹⁶O-AgBr, ²⁸Si-AgBr and ³²S-AgBr interactions at 4.5A GeV/c have been presented in table 3 along with the corresponding experimental values. From the table it is seen that for the UrQMD simulated events also the generalized fractal dimension D_q decrease with order q signifying the presence of multifractality for the simulated events. But the values of D_q for the simulated events are lower than the corresponding experimental counterparts for all the interactions. The variation of D_q with order q has been shown in figure 2 for ¹⁶O-AgBr, ²⁸Si-AgBr and ³²S-AgBr interactions. As in the case of experimental data in case of simulated data also we have calculated the values of $\frac{d_q}{d_2}$ and presented the values in table 4. From the table it may be

noticed that the experimentally obtained values of $\frac{d_q}{d_2}$ are little higher than the corresponding UrQMD simulated values.

To quantify the multifractality in case of UrQMD simulated data we have studied the variation of $\frac{d_q}{d_2}$ with order q in figure 3 for $^{16}\text{O-AgBr}$, $^{28}\text{Si-AgBr}$ and $^{32}\text{S-AgBr}$ interactions. From the slope of the plot of $\frac{d_q}{d_2}$ against q we have calculated the value of r which signifies the degree of multifractality. The extracted value of r has been presented in table 5 for the UrQMD simulated events. From the table it may be seen that the r value characterizing the degree of multifractality calculated for the UrQMD simulated events are lower than the corresponding experimental value for all the three interactions. This observation signifies the presence of stronger multifractality for the experimental data. We have studied the variation of D_q against $\frac{\ln q}{(q-1)}$ in figure 4 for the UrQMD data sample of $^{16}\text{O-AgBr}$, $^{28}\text{Si-AgBr}$ and $^{32}\text{S-AgBr}$ interactions in order to calculate the multifractal specific heat. From the best linear behavior of the plotted points the multifractal specific heat for the UrQMD data sample have been evaluated and presented in table 6. From the table it may be seen that the values of the multifractal specific heat for the experimental and simulated data agrees reasonably well with each other.

Discussion on Systematic Errors

Earlier we have mentioned that the errors shown in all the plots and tables are statistical errors only. Apart from statistical error, estimation of systematic errors is also important. Detailed analysis on systematic errors for the same data set has been presented in our earlier publication [41-43]. From our previous papers [41-43], we find that the efficiency of track finding and pion identification contribute to the systematic error of the analysis. It has been mentioned in [41-43] that applying the “along the track” scanning procedure with the help of two independent observers helps us to increase the scanning efficiency to more than 99% and hence to minimize the systematic errors to less than 1%. It has been mentioned in [41-43] that “along the track” scanning method gives reliable event samples because of its high detection efficiency. In nuclear emulsion detector tracks of e^+e^- pair originating from γ -conversion may cause problem in pion identification [41-43]. These tracks are produced at a distance from the interaction point after travelling through certain radiation lengths. In order to exclude such tracks lying close to shower tracks near vertex, special care was taken while

performing angular measurements. Usually all the shower tracks in the forward direction were followed more than 100–200 μm from the interaction vertex for angular measurement. The tracks due to e^+e^- pair can be easily recognized from the grain density measurement, which is initially much larger than the grain density of a single shower track. It may also be mentioned that the tracks of an electron and positron when followed downstream in nuclear emulsion showed considerable amount of Coulomb scattering as compared to the energetic charged pions. Such e^+e^- pairs were eliminated from the data and consequently they contribute almost nothing ($\sim 0.01\%$) to the systematic errors [41-43].

It has been mentioned earlier that the shower particles are mostly pions (more than 90%) with a small proportion (less than 10%) of kaons and hyperons among them. The presence of K-mesons, hyperons and any other mesons among the pions are treated as contaminations. The level of contamination due to the presence of kaons and hyperons varies with the projectile beam, target nucleus as well as with the incident energy. As nuclear emulsion track detector cannot distinguish between pions and other mesons or hyperons, one possible source of systematic errors is the presence of such contaminations among the pions. Estimation of percentage of contaminations among the pions in nuclear emulsion at the specific energy can be done by applying any event generator [41-43]. UrQMD model can serve this purpose satisfactorily. On UrQMD simulation along with pions K-mesons, ϕ -mesons, Λ -hyperons and η mesons are also produced. All these mesons can easily be distinguished in terms of their specific codes available from the UrQMD output. Applying the UrQMD model it has been seen that [41-43] for ^{16}O -AgBr, ^{28}Si -AgBr and ^{32}S -AgBr interactions, above 90% of the produced particles are π -mesons, (3-5) % of the produced particles are kaons and (1-2) % of the produced particles are ϕ -mesons, Λ -hyperons and η mesons. In our earlier publication [41-43], we have also calculated expected values of average multiplicity of the pions only for all the interactions if the number of other mesons and hyperons could have been evaluated experimentally. We have seen from [41-43] that if we can distinguish between the pions and other mesons as well as Λ -hyperons, the average multiplicity of only the pions would have been $16.68 \pm .23$, $21.58 \pm .27$ and $25.54 \pm .24$ ^{16}O -AgBr, ^{28}Si -AgBr and ^{32}S -AgBr interactions respectively [41-43]. The contribution to the systematic errors due to the presence of other mesons and hyperons with the pions in the shower particles has been

calculated to be $(7.60 \pm 0.05$ to $8.91 \pm 0.07)$ % for these interactions. Therefore, the total contribution of systematic errors in our analysis does not exceed 10% [41-43].

Conclusions and Outlook

To summarize we may recall that in this paper we have presented an analysis of multifractality and multifractal specific heat in the frame work of Renyi entropy analysis for the produced shower particles in nuclear emulsion detector for ^{16}O -AgBr, ^{28}Si -AgBr and ^{32}S -AgBr interactions at 4.5A GeV/c. Experimental results have been compared with the prediction of UrQMD model. Qualitative information about the multifractal dynamics of particle production process have been extracted and reported in the present analysis. The emulsion technique allows us to observe these systems to the smallest details and gives the possibility of studying them experimentally.

The significant conclusions of this analysis are as follows.

1. Renyi entropy values of all the interactions decrease with the order number q for both experimental and UrQMD simulated data. Renyi entropy values for UrQMD data are less than the corresponding experimental values.
2. Generalized fractal dimension calculated from Renyi entropy for both experimental and UrQMD simulated data decrease with the increase of order q suggesting the presence of multifractality in multi particle production process.
3. Degree of multifractality is found to be higher for the experimental data in comparison to the simulated data and it increases with the increase of projectile mass.
4. Multi fractal specific heat for the simulated data agrees well with the experimental data except for interactions.

It is true that there are many papers available in the literature where presence of multifractality has been tested experimentally in multiparticle production in high energy nucleus-nucleus interactions by different methods. But the method adopted in this paper to study multifractality seems to be interesting and in this regard our study deserves attention. The observed multifractal behaviour of the produced shower particles may be viewed as an experimental fact.

References

- [1] S. Dutta et al Physica A 396(2014)155
- [2] S. Dutta et al Physica A 463(2016)188
- [3] S. Dutta et al Physica A 491(2018)188
- [4] X. Jiang et al Fractals 25(2017) 1750052
- [5] Zhi-Qiang Jiang et al Fractals 25(2017) 1750054
- [6] B.B. Mandelbrot, The Fractal Geometry of Nature, Freeman, New York, 1982
- [7] Z.Chen et al Phy Rev E 65(2002)041107
- [8] R. C. Hwa, Phys. Rev. D 41 (1990) 1456.
- [9] R. C. Hwa and J. Pan Phys. Rev. D 45(1992) 1476
- [10] F. Takagi, Phys.Rev. Lett. 72 (1994) 32
- [11] R.Saha, A.Deb and D.Ghosh Can.J.Phys. 95 (2017) 699
- [12] N. Parashar, J. Phys. G 22 (1996) 59.
- [13] M. I. Adamovich et al. (EMU01 Collaboration), Europhys. Lett. 44 (1998) 571.
- [14]. M. K. Ghosh, A. Mukhopadhyay and G. Singh, J. Phys. G 32 (2006) 2293.
- [15] S. Ahmad and M. A. Ahmed, J. Phys. G 32 (2006) 1279
- [16]. S. Bhattacharyya et al, Physica A 390 (2011) 4144
- [17] Shakeel Ahmad et al Chaos, Solitons and Fractals 42(2009)538
- [18] D. Ghosh et al Can. Jour . of Phys. 83(2005)1169
- [19] A. Kamal et al Int. Jour. of Mod. Phy E 23 (2014)1450016
- [20] S. Bhattacharyya, M.Haiduc, A.T. Neagu and E. Firu Fractals 26(2018)1850015
- [21] S.Dutta et al Int. Jour of Mod. Phy A 29(2014)1450084
- [22]Y.X.Zhang et al Int. Jour of Mod. Phy A 23(2008)2809
- [23] S. Bhaduri and D. Ghosh Mod. Phy. Lett A 31(2016)1650158
- [24] S. Bhaduri and D. Ghosh Eur.Phys.J. A53 (2017) 135
- [25] G. Bhoumik et al Advances in High energy Phys. 2016(2016)7287803
- [26] P. Mali et al Phys. A 450 (2016)323
- [27] P. Mali et al Phy. A 493(2018) 253
- [28] P.Mali et al Chaos, Solitons and Fractals 94(2017)86
- [29] P. Mali et al Mod. Phy. Lett A 32(2017)1750024
- [30] P. Mali et al Physica A 424 (2015) 25
- [31] P. Mali et al Mod. Phy. Lett A 32(2017)1750024

- [32] P. Mali et al Physica A 424 (2015) 25
- [33] A. Renyi "On Measurements of Entropy and Information", in Proc. 4th Berkeley Symp on Math. Stat. Prob. 1960 Vol.1, University of California Press, Berkeley , Los Angeles 1961, page 547
- [34] C Beck and F. Schloegl " Thermodynamics of Chaotic Systems", Cambridge University press 1993
- [35] I.M. Dremin and J.W. Gary Phys. Rep. 349(2001)313
- [36] A. Białas and W. Czyz', Phys. Rev. D 61(2000) 074021
- [37] A. Białas and W. Czyz', Acta Phys. Pol.B 31(2000) 687
- [38] A. Białas and W. Czyz', Acta Phys. Pol.B 31(2000) 2803
- [39]. M. Pachr et al., Mod. Phys. Lett. A7 (1992) 2333.
- [40]. A. Mukhopadhyay et al., Phys. Rev. C47 (1993) 410.
- [41] S. Bhattacharyya, M.Haiduc, A.T. Neagu and E. Firu Jour. of Phys G 40(2013)025105
- [42] S. Bhattacharyya, M.Haiduc, A.T. Neagu and E. Firu, Phys. Letter B 726, (2013) 194.
- [43] S. Bhattacharyya, M.Haiduc, A.T. Neagu and E. Firu, Jour. Phys. G 41, (2014) 075106.
- [44] M.I.Adamovich et al., EMU01 Collaboration, Phys. Lett. B 227, (1989) 285 .
- [45] P. Mali, A. Mukhopadhyay and G. Singh , Phys Scripta 85 (2012) 065202.
- [46] S. Bhattacharyya, M.Haiduc, A.T. Neagu and E. Firu Can.J.Phys. 95 (2017) 715
- [47] M.K Ghosh et al Can. J. Phys. 88: (2010) 575
- [48] L.D. Landau, E.M. Lifshitz, Statistical Physics, Part I, Pergamon Press, 1980, p. 28.
- [49] A. Bershadskii, Phys. Rev. C 59 (1999) 364.
- [50] H.E. Stanley, P. Meakin, Nature 335 (1988) 405.
- [51] A. De Wolf, I.M. Dremin, W. Kittel, Phys. Rep. 270 (1996) 48.
- [52] R. Peschanski, Int. J. Mod. Phys. A 6 (1991) 3681.
- [53] M. Bleicher et al Jour. of Phys. G. 25 (1999) 1859
- [54] S. A. Bass et al Prog. Part. Nucl. Phys. 41 (1998) 255

Acknowledgement

The authors are grateful to Prof. Pavel Zarubin, JINR, Dubna, Russia for providing them the required emulsion data. Dr. Bhattacharyya acknowledges Prof. Dipak Ghosh, Department of Physics, Jadavpur University and Prof. Argha Deb Department of Physics, Jadavpur University, for their inspiration in the preparation of this manuscript.

Table 1

Interactions	Average Multiplicity	
	Experimental	UrQMD
$^{16}\text{O-AgBr}$ (4.5AGeV/c)	18.05 ± 0.22	17.79 ± 0.21
$^{28}\text{Si-AgBr}$ (4.5AGeV/c)	23.62 ± 0.21	27.55 ± 0.22
$^{32}\text{S-AgBr}$ (4.5AGeV/c)	$28.04 \pm .14$	30.84 ± 0.17

Table 1 represents the average multiplicities of the shower particles for all the interactions in case of the experimental and the UrQMD data.

Table 2

Interactions	Order	Experimental values of Renyi Entropy H_q	UrQMD simulated values of Renyi Entropy H_q
$^{16}\text{O-AgBr}$	2	$3.47 \pm .002$	$3.05 \pm .003$
	3	$3.41 \pm .003$	$2.99 \pm .004$
	4	$3.37 \pm .002$	$2.95 \pm .002$
	5	$3.34 \pm .002$	$2.92 \pm .002$
$^{28}\text{Si-AgBr}$	2	$3.76 \pm .002$	$3.29 \pm .003$
	3	$3.69 \pm .002$	$3.21 \pm .002$
	4	$3.63 \pm .003$	$3.17 \pm .002$
	5	$3.59 \pm .003$	$3.13 \pm .003$
$^{32}\text{S-AgBr}$	2	$.834 \pm .004$	$3.36 \pm .004$
	3	$.815 \pm .007$	$3.28 \pm .003$
	4	$.793 \pm .008$	$3.24 \pm .003$
	5	$.777 \pm .008$	$3.20 \pm .002$

Table 2 represents the experimental and UrQMD simulated values of Renyi Entropy H_q for $^{16}\text{O-AgBr}$, $^{28}\text{Si-AgBr}$ and $^{32}\text{S-AgBr}$ interactions at 4.5AGeV/c.

Table 3

Interactions	Order	Experimental values of Generalized fractal dimension $\mathbf{D_q}$	UrQMD simulated values of Generalized fractal dimension $\mathbf{D_q}$
$^{16}\text{O-AgBr}$	2	$.892 \pm .007$	$.826 \pm .002$
	3	$.877 \pm .006$	$.810 \pm .003$
	4	$.866 \pm .009$	$.799 \pm .004$
	5	$.858 \pm .008$	$.791 \pm .005$
$^{28}\text{Si-AgBr}$	2	$.897 \pm .004$	$.829 \pm .002$
	3	$.880 \pm .004$	$.808 \pm .002$
	4	$.866 \pm .007$	$.798 \pm .004$
	5	$.857 \pm .007$	$.788 \pm .005$
$^{32}\text{S-AgBr}$	2	$.924 \pm .004$	$.836 \pm .003$
	3	$.907 \pm .007$	$.815 \pm .004$
	4	$.896 \pm .008$	$.805 \pm .005$
	5	$.884 \pm .008$	$.796 \pm .006$

Table 3 represents the experimental and UrQMD simulated values of Generalized fractal dimension $\mathbf{D_q}$ for $^{16}\text{O-AgBr}$, $^{28}\text{Si-AgBr}$ and $^{32}\text{S-AgBr}$ interactions at 4.5AGeV/c.

Table 4

Interactions	Order	Experimental values of $\frac{d_q}{d_2}$	UrQMD simulated values of $\frac{d_q}{d_2}$
$^{16}\text{O-AgBr}$	2	$1.00 \pm .02$	$1.00 \pm .03$
	3	$1.14 \pm .03$	$1.09 \pm .02$
	4	$1.24 \pm .05$	$1.15 \pm .03$
	5	$1.31 \pm .05$	$1.20 \pm .04$
$^{28}\text{Si-AgBr}$	2	$1.00 \pm .02$	$1.00 \pm .02$
	3	$1.16 \pm .03$	$1.12 \pm .02$
	4	$1.30 \pm .05$	$1.18 \pm .03$
	5	$1.39 \pm .06$	$1.24 \pm .04$
$^{32}\text{S-AgBr}$	2	$1.00 \pm .02$	$1.00 \pm .02$
	3	$1.22 \pm .04$	$1.13 \pm .03$
	4	$1.37 \pm .04$	$1.19 \pm .03$
	5	$1.53 \pm .08$	$1.24 \pm .04$

Table 4 represents the experimental and UrQMD simulated values of $\frac{d_q}{d_2}$ for $^{16}\text{O-AgBr}$, $^{28}\text{Si-AgBr}$ and $^{32}\text{S-AgBr}$ interactions at 4.5A GeV/c.

Table 5

Interactions	r value characterizing the degree of multifractality obtained from the plot $\frac{d_q}{d_2}$ with order number q	
	Experimental	UrQMD
¹⁶ O-AgBr (4.5AGeV/c)	.206 ± 0.011	.132 ± 0.006
²⁸ Si-AgBr (4.5AGeV/c)	.262 ± .011	.156 ± 0.017
³² S-AgBr (4.5AGeV/c)	.348 ± .014	.156 ± 0.019

Table 5 represents the **r** value characterizing the degree of multifractality obtained from the plot $\frac{d_q}{d_2}$ with order number q for ¹⁶O-AgBr, ²⁸Si-AgBr and ³²S-AgBr interactions at 4.5AGeV/c in case of experimental and simulated events.

Table 6

Interactions	Multifractal Specific heat	
	Experimental	UrQMD
¹⁶ O-AgBr (4.5AGeV/c)	.116 ± 0.004	.119 ± 0.003
²⁸ Si-AgBr (4.5AGeV/c)	.138 ± .007	.138 ± .005
³² S-AgBr (4.5AGeV/c)	.133 ± .010	.136 ± .004

Table 6 represents the values of multifractal specific heat of the produced shower particles in ¹⁶O-AgBr, ²⁸Si-AgBr and ³²S-AgBr interactions at 4.5AGeV/c in case of experimental and simulated events.

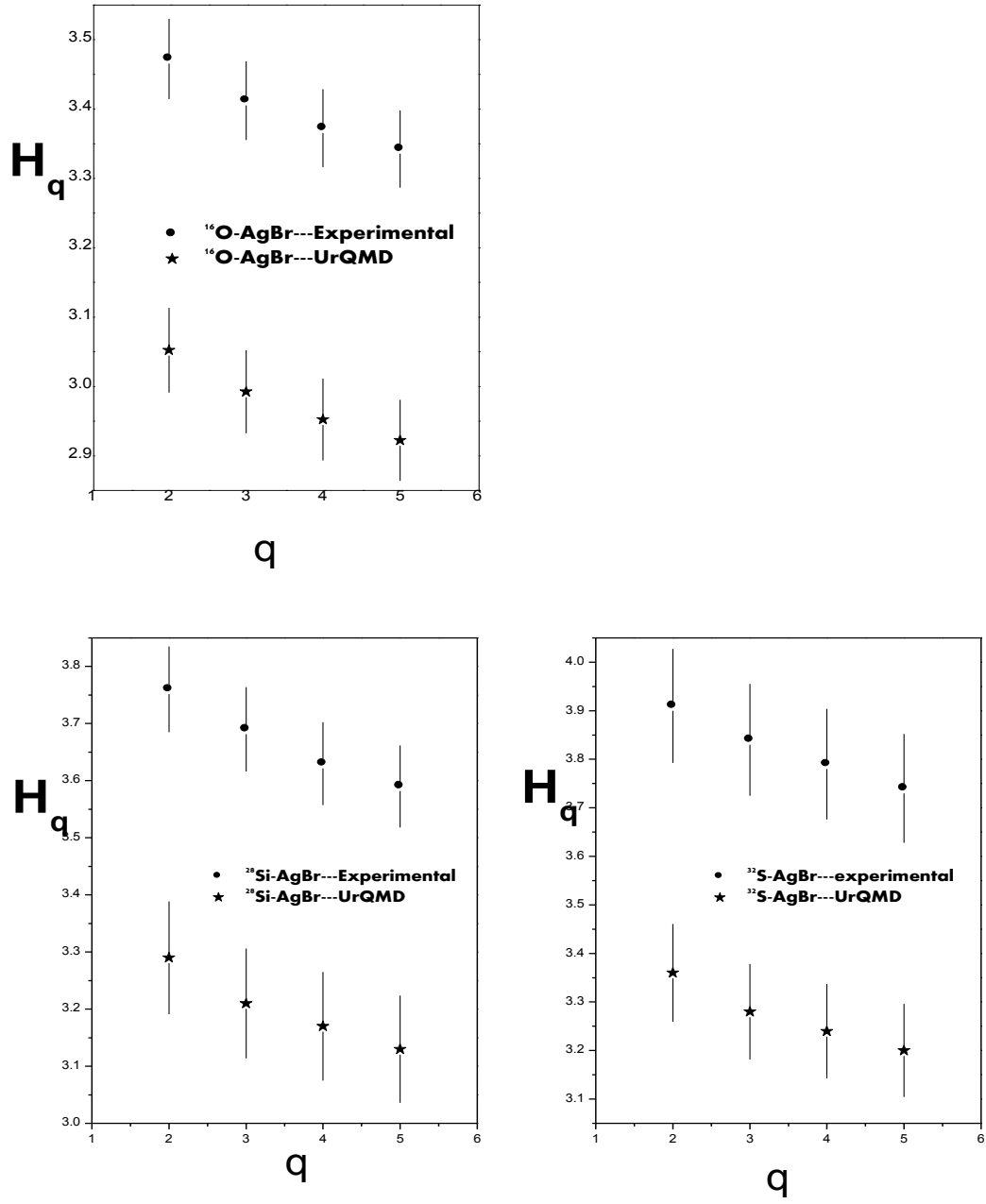


Figure 1 represents the variation of Renyi entropy with order number q for $^{16}\text{O-AgBr}$, $^{28}\text{Si-AgBr}$ and $^{32}\text{S-AgBr}$ interactions at 4.5 AGeV/c in case of experimental and simulated events.

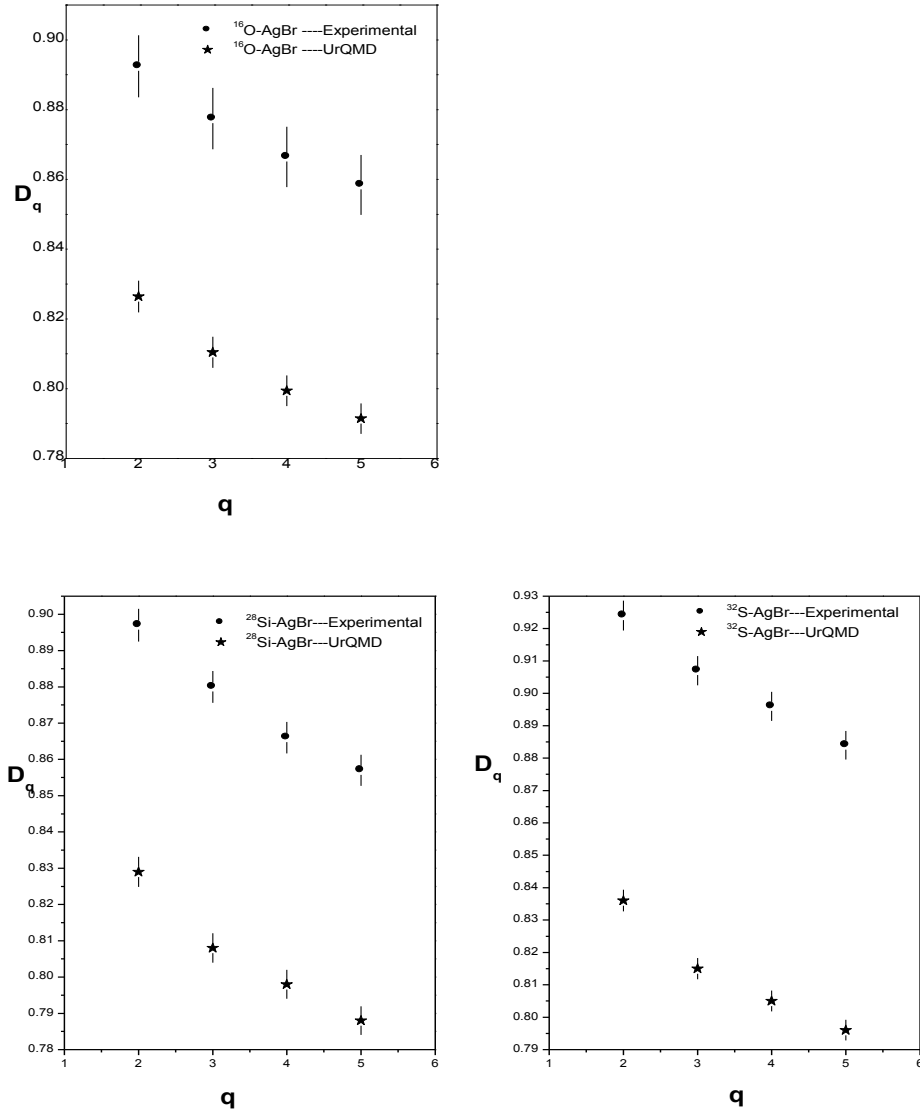


Figure 2 represents the variation of generalized fractal dimension with order number q for $^{16}\text{O-AgBr}$, $^{28}\text{Si-AgBr}$ and $^{32}\text{S-AgBr}$ interactions at 4.5A GeV/c in case of experimental and simulated events.

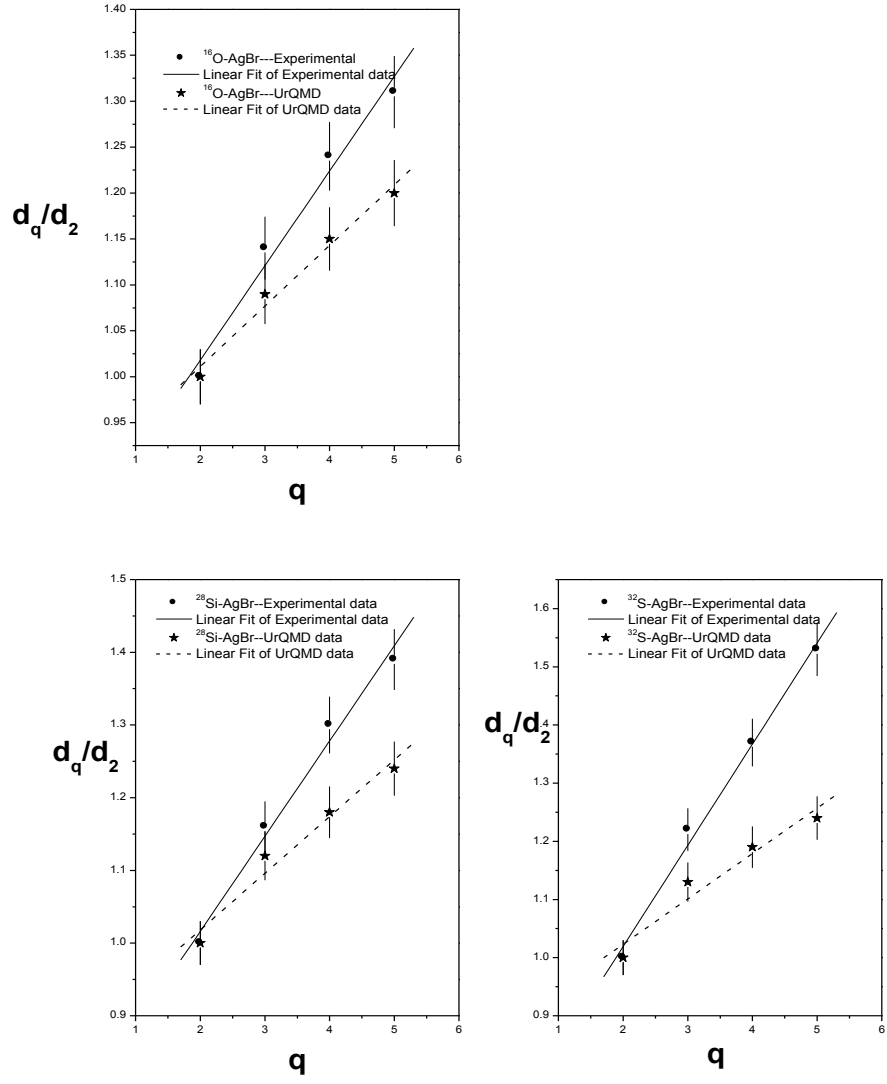


Figure 3 represents the variation of $\frac{d_q}{d_2}$ with order number q for $^{16}\text{O-AgBr}$, $^{28}\text{Si-AgBr}$ and $^{32}\text{S-AgBr}$ interactions at 4.5A GeV/c in case of experimental and simulated events.

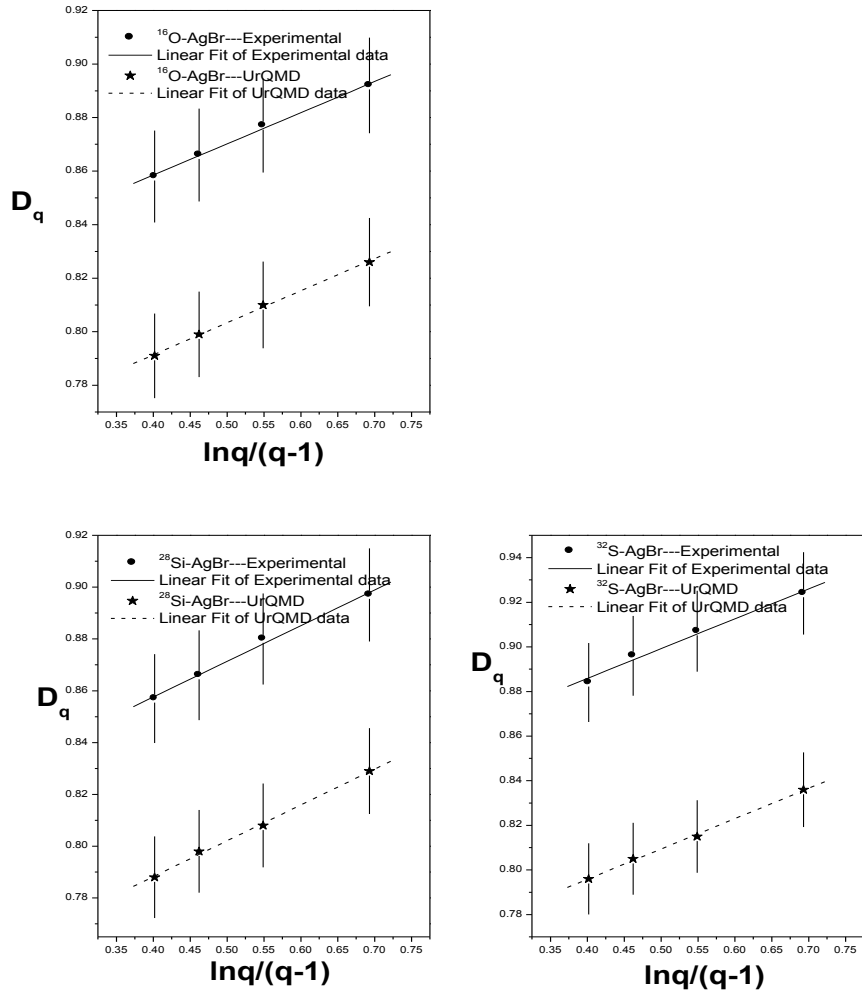


Figure 4 represents the variation of D_q against $\frac{\ln q}{(q-1)}$ for $^{16}\text{O-AgBr}$, $^{28}\text{Si-AgBr}$ and $^{32}\text{S-AgBr}$ interactions at 4.5 AGeV/c in case of experimental and simulated events.